S.V. SOLOGUB,[1] I.V. BORDENJUK,[1] C. TEGENKAMP,[2] H. PFNÜR[2]

[1] Institute of Physics, Nat. Acad. of Sci. of Ukraine
(46, Nauky Ave., Kyiv 03680, Ukraine; e-mail: sologub@iop.kiev.ua)
[2] Institut für Festkörperphysik, Leibniz Universität Hannover
(2, Appelstraße, Hannover 30167, Germany)

SURFACE SCATTERING OF CHARGE CARRIERS AND SURFACE ELECTRONIC STATES

Experimental researches of the charge carrier scattering at Mo(110) and W(110) surfaces atomically clean or covered with a hydrogen (deuterium) monolayer with the participation of surface electronic states are considered. In addition, the scattering mechanisms of charge carriers in spin-polarized surface electronic states in Bi(111) epitaxial nanofilms with the atomically clean surface or the surface covered with magnetic and nonmagnetic adatoms to low coverages are discussed.

K e y w o r d s: surface scattering of charge carriers, surface electronic states, electron-hole Umklapp processes, bismuth epitaxial nanofilms, semimetal-semiconductor transition, Rashba effect, magnetotransport phenomenon.

1. Introduction

Functional parameters of modern electronic devices depend to a great extent on the electron transport properties of low-dimensional conductors, which, in turn, depend on the charge carrier scattering by the surface, in particular, on the scattering of charge carriers in surface electronic states. Stimulating examples inspiring the further development of researches in this direction include the practical application of the huge magnetoresistance effect based on the spin-dependent surface scattering [1] and a fascinating prospect of using the materials with strong spin-orbit coupling, in which the scattering of surface-state carriers is suppressed or even forbidden. Topological insulators (TIs) are the most striking group in this class of materials. They are multicomponent compounds with a dielectric volume and conducting spin-split surface electronic states [2]. Charge carriers in them are topologically protected from the scattering [3]. Unlike the traditional way where the conductivity is increased by reducing the surface scattering diffuseness, the application of TIs may become an essentially new approach, which will ideally allow one to get rid of the carrier scattering in general. Another representative of surface systems with strong spin-orbit coupling is thin Bi films, in which the spin-split conducting surface electronic states

dominate as a result of the quantum size effect: the semimetal-semiconductor transition in the material bulk [4]. Therefore, the thin epitaxial Bi nanofilms, which are an object of our researches, are a convenient and simple enough model system for studying the scattering processes of surface-state carriers in TIs.

In classical conductors, the contribution of the surface scattering to transport properties becomes substantial, when at least one of their dimensions, d, becomes comparable with the mean free path of charge carriers, l ($d \leqslant l$). Therefore, the domination of the surface scattering can be achieved by decreasing the temperature, using superpure materials with a perfect crystal structure, and also by applying a strong magnetic field, which concentrates the electric current near the conductor surface [5]. This experimental approach was applied by us to elucidate the role of surface electronic states at the scattering of charge carriers by the metal surface. Those researches of the adsorption allowed us to resolve the contribution of surface electronic states to the macroscopic magnetoresistance (MR) of a metal against the background of the contribution made by the electron states in the bulk, this task being considered rather problematic till now [6].

In this work, we propose a brief review of our low-temperature ultrahigh-vacuum magnetotransport researches of physical effects governed by the surface scattering of charge carriers and the properties of surface electronic states, whose parameters are mod-

ified by the submonolayer adsorption. First, we consider galvanomagnetic dimensional researches, aimed at studying the role of surface electronic states in the scattering of charge carriers by the atomically clean or hydrogen-covered (to a monolayer) single-crystalline W(110) and Mo(110) surfaces [7–9]. The discussed experiments were carried out at the Institute of Physics of the NAS of Ukraine (Kyiv). In the second part of the review, we discuss the results of researches of the (magneto)transport that concern the scattering of carriers in spin-polarized surface electronic states of epitaxial Bi(111) films at ultra-thin coverages of adsorbed magnetic and nonmagnetic atoms [10–13]. This series of experiments was carried out at the Institut für Festkörperphysik of the Leibniz Universität (Hannover).

2. Transitions between Surface and Bulk Electronic States at Charge Carrier Scattering by (110) Tungsten and Molybdenum Surfaces

Regularities in the surface scattering of charge carriers at the surface of perfect metal single crystals were formulated by Andreev [14] in the form of conservation laws for the energy,

$$\varepsilon = \varepsilon' = \varepsilon_F, \tag{1}$$

$$\mathbf{k}_t = \mathbf{k}'_t + n\mathbf{g}, \tag{2}$$

where ε is the carrier energy, ε_F the Fermi energy in the metal, $\mathbf{k}_t$ the tangential component of the carrier wave vector, $\mathbf{g}$ an arbitrary vector of the reciprocal surface lattice, n any integer, and the primed and nonprimed quantities are related to the carrier state before and after the scattering, respectively. Equations (1) and (2) describe the model of surface scattering as the diffraction of electron waves at the surface, when the scattering is determined by the symmetry of the metal surface lattice and the topology of its Fermi surface projection on the plane of a scattering surface. The validity of this concept was confirmed by experimental researches of the surface scattering at atomically clean or covered with adsorbates (to a submonolayer) surfaces of single-crystalline refractory metals, which were carried out, by using the methods based on galvanomagnetic size phenomena [5, 15].

In the framework of the diffraction model, changes in MR of thin ($d \sim 0.1$ mm) single-crystalline W(110)
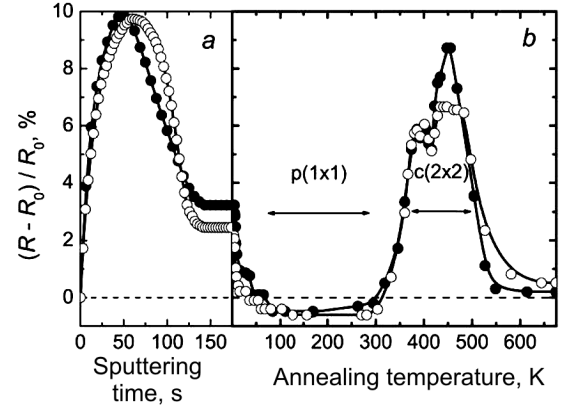

Fig. 1. Changes of the Mo(110) plate magnetoresistance: (*a*) at the hydrogen and deuterium adsorption on a plate cooled down to $T = 4.2$ K, (*b*) at the stepwise annealing of sputtered films of adsorbates. Hollow circles correspond to hydrogen, and solid circles to deuterium; arrows point to the probable regions of existence of adsorbate submonolayer lattices [9]

and Mo(110) plates, which are under the conditions of static skin effect (i.e. when a strong, in the classical meaning, magnetic field is applied in the surface plane perpendicularly to the surface current and, owing to the surface scattering, stimulates the current to concentrate in the near-surface layer with a thickness of the order of the Larmor radius [16]), can be interpreted as a result of the hydrogen (H) (or deuterium (D)) submonolayer adsorption. Below, we consider experimental results that characterize adsorption systems (H,D)–Mo(110) [9]. However, similar effects were also revealed by us in adsorption systems (H,D)–W(110) [7, 8].

Figure 1 demonstrates that the adsorption of H(D) on the Mo(110) surface at $T = 4.2$ K gives rise to the increase of the plate MR stemming from a gradual symmetry violation of the atomically clean Mo(110) surface, when adcenters are randomly filled to a coverage of about 0.5 ML (monolayer). The MR decrease is connected with a gradual symmetry restoration of the atomically clean surface by creating the domains with monolayer structure (1×1) by means of filling the free adsorption centers to a coverage of about 1 ML. Hence, first, the diffuseness of the charge carrier scattering increases; then, after the surface coverage reaches 0.5 ML, the surface specularity starts to grow [17].

The stepwise annealing of H(D) films sputtered at $T = 4.2$ K brings about a nonmonotonic change of
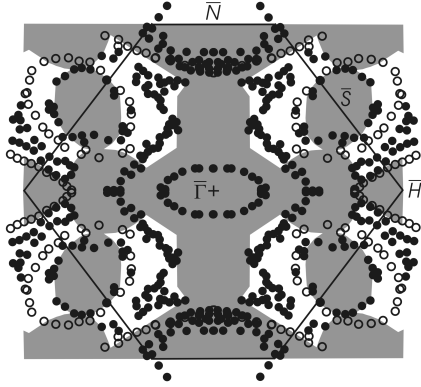
Fig. 2. Shadow projection of the Fermi surface of Mo bulk electron states onto the plane (110) (tinted region); the structure of the surface electronic states of the atomically clean Mo(110) surface (black circles) and of the same surface but covered with an ordered monolayer of hydrogen (hollow circles) [19]

MR, which is a result of the partial desorption of adatoms and the formation of their submonolayer lattices (Fig. 1, *b*). The annealing was carried out for about 1 s at every temperature point; then, the temperature was decreased to the helium one, and the MR was measured. The formation of surface lattices from adsorbates (except for the (1×1) structure, which reproduces the lattice of the atomically clean surface) changes the surface symmetry and, in accordance with Eq. (2), can affect the character of the surface scattering. In particular, as was shown experimentally in work [15] for the first time and confirmed in subsequent experiments [5], the largest variations in MR occur, when the channels of the electron-hole Umklapp, i.e. the charge carrier transitions between the electron and hole sections on the Fermi surface, are made "opened" or "closed". For example, the increase of MR at the annealing (Fig. 1, *b*; $T \approx 450$ K) was induced just by electron-hole transitions, which became allowed at the formation of the $c(2 \times 2)$ structure.

At annealing temperatures $T > 100$ K (Fig. 1, *b*), the ordering in monolayer (1×1)-H(D) lattices takes place; the latter reproduce the symmetry of the atomically clean Mo(110) surface and expectedly invoke a reduction of MR and the surface scattering. A constant MR value in the interval 100 K $< T <$ 300 K testifies to the maximum ordering and the constant concentration of adsorbates in the (1×1)-H(D) lattices. Unexpected and intriguing is the absolute value

of MR for a Mo(110) plate covered with an ordered monolayer of H(D) adatoms. It is lower than the value typical of a plate with the atomically clean surface! In other words, an ordered monolayer of adsorbed atomic hydrogen (deuterium) increases the specularity of the charge carrier surface scattering!

Note that this effect is observed against the background of factors that increase the scattering diffuseness. In particular, the cross-sections of the charge carrier scattering by hydrogen (deuterium) adatoms and surface Mo atoms are strongly different. The adatom lattice (1×1)-H(D) is shifted in the lateral plane with respect to the upper lattice of Mo atoms. In addition, owing to the existence of two equivalent adsorption centers with the threefold coordination [18], (1×1)-H(D) films consist of domains of two types and contain numerous domain walls. Note also that the absence of a Mo(110) surface reconstruction at the adsorption of (1×1)-H(D) monolayers [18] does not allow the found specific effect to be related with the surface reconstruction.

The effect origin becomes clear if we consider a transformation of the structure of electronic states at the Mo(110) surface owing to the adsorption of a (1×1)-H(D) monolayer. This process was experimentally studied, by using the angle-resolved photoemission spectroscopy (ARPES) method (Fig. 2) [19]. (The results of similar researches for (1×1)-H(D) monolayers adsorbed on the W(110) surface [20] were used by us, while analyzing the system (H,D)–W(110) [7, 8].)

The graphic interpretation of the conservation laws (1) and (2) ($n\mathbf{g} = 0$) means that the transitions between surface and bulk electronic states are possible if the projections of the Fermi contours of surface states and the Fermi surfaces of bulk states onto the plane of the scattering surface overlap (at equilibrium, the surface and bulk states have the same energy $\varepsilon_{\mathrm{F}} \pm k_{\mathrm{B}}T$). Such transitions are typical of the atomically clean Mo(110) surface. For example (Fig. 2), the transitions are allowed between the Fermi contours centered at the points $\bar{\Gamma}$ and $\bar{N}$ of the surface Brillouin zone and, respectively, the electron jack and the hole octahedron of the bulk Fermi surface. They comprise a version of the multichannel specular scattering of charge carriers at the surface [5, 15].

The adsorption of a hydrogen monolayer and its ordering result in that some Fermi contours of surface states disappear (e.g., those centered at the point

$\bar{\Gamma}$), and the others emerge (e.g., those centered at the point $\bar{H}$). In addition, some Fermi contours (e.g., those centered at the points $\bar{S}$) are "squeezed out" beyond the boundaries of the bulk Fermi surface projection. Such transformations result in the prohibition of transitions between the surface and bulk states, and stimulate an enhancement of the surface scattering specularity. The fact that the MR variation caused by this effect is not too large is associated with the small phase volume occupied by the surface electronic states in the momentum space (Fig. 2). Moreover, the increase in the specularity is actually much larger, because it is observed against the background of a number of the mentioned factors that increase the surface scattering diffuseness. At last, even in the case of thin perfect single-crystalline plates of metals under the conditions of the static skin effect, the contribution of the surface component to the conductance can be observed against a considerable conductance of the metal bulk.

3. Scattering of Charge Carriers in the Spin-Polarized Surface Electronic States of Bismuth

Specific properties of semimetallic Bi – an extremely large Fermi wavelength ($\lambda_{\mathrm{F}} \approx 30$ nm), a small effective mass (about $0.001m_e$), a high mobility of charge carriers, the concentration of carriers in the surface electronic states (about 10^{13} cm^{-2}) dominating over that of carriers in the bulk (10^{17} cm^{-3}), and the strong spin-orbit coupling—form the basis for a number of bright physical effects inherent to this substance [21–24]. The quantum-mechanical size effect is one of them, which is responsible for the semimetal-semiconductor transition in the bulk of thin Bi films ($d < 30$ nm) [3, 22]. In this case, the electric conductivity in the film bulk can be neglected at low temperatures ($T < 60$ K [10]), so that the main channel of charge transfer is determined by the surface electronic states of Bi. It was experimentally confirmed, in particular, for epitaxial Bi films grown up on the Si(111) surface [25, 26]. Moreover, using the method of angle- and spin-resolved photoemission spectroscopy, it was found that, owing to the Rashba effect (elimination of the spin degeneration in systems with strong spin-orbit coupling, because its spatial inversion symmetry becomes broken owing to the presence of the surface [27]), the surface electronic states of Bi, in particular,

of the Bi(111) surface [28], are spin-polarized [29–31]. From the viewpoint of the practical application in electronics and spintronics, a special interest is attracted by nontrivial properties of the electron transport in spin-split electronic states, namely, the prohibition of the charge carrier scattering in the direction opposite to the carrier motion one (backward). As a result of the time inversion symmetry, this scattering is possible only if the carrier changes the direction of its spin, e.g., at its scattering by a magnetic impurity.

In this section, we present a brief review of (magneto)transport researches dealing with the processes of carrier scattering in spin-split surface electronic states of epitaxial Bi(111) films, the properties of which were modified by adsorbing the low (< 0.01 ML) concentrations of nonmagnetic and magnetic impurities (Bi, Sb, Co, Fe, Tb, and Cr atoms) [10–13].

In our researches, we used Bi films grown up on the Si(111)-7 × 7 substrate. The film thickness was equal to 20 BL (bilayer, 1 BL ≈ 3.9 nm), which is optimal for the electron transport through the surface electronic states to dominate [10]. The surface of Bi(111) films demonstrated the well-resolved spots of low-energy electron diffraction with weak attributes of the rotational disordering of crystallites. A typical conductance value, G_0, for 20-BL films with the atomically clean surface amounted to 2.0 ± 0.3 mS [11]. The analysis of the full width at the half maximum of the (00) diffraction spot, which was measured at various electron energies (the so-called H(S) analysis [32]), showed that the average size of terraces (domains) on the film surface amounted to about 15 nm [11, 12]. Therefore, even at adsorbate coverages $\delta\Theta \geqslant$ $\geqslant 0.001$ ML, the mean free path of charge carriers was determined by their scattering at adatoms (the distance between adatoms can be evaluated as $1/\sqrt{\delta\Theta}$, where $\delta\Theta$ is the absolute adsorbate concentration).

Figure 3 demonstrates the relative variation of the conductance, $\Delta G/G_0 = G(\delta\Theta)/G_0 - 1$, of the Bi(111) film when the low concentrations of (semi)metals ($\delta\Theta = (0 \div 0.1)$ ML) are adsorbed on its surface. If $\delta\Theta > 0.05$ ML, a strong reduction of the conductance is observed, resulting from the non-coherent scattering of carriers by adsorbed impurities. This fact is another evidence of the dominating contribution made by surface electronic states to the electron transport in Bi(111) films. The nonmonotonic behavior of $\Delta G/G$ at ultrathin Tb and Cr coverages [12, 13] testifies to a considerable mobility of adatoms even
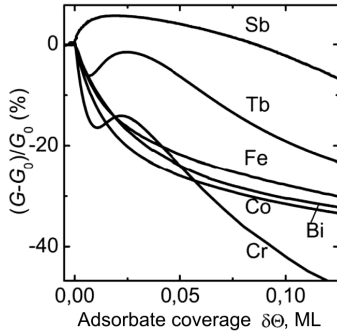
Fig. 3. Variations of the electric conductance of a 20-ML Bi(111) film adsorbing various magnetic and nonmagnetic adatoms on its surface; $T = 10$ K, G_0 is the conductance of the film with atomically clean surface

at $T = 10$ K. It is a result of the competition between the processes of charge redistribution between adatoms and surface states, on the one hand, and the scattering of their charge carriers, on the other hand. The numerical simulation on the basis of a theoretical model that involves the processes of adsorption, adsorbate diffusion, adsorbate capture by domain walls, formation of adatom islands, and charge redistribution between them and the surface states allowed us to reproduce the experimental dependence of the conductance variation at the Tb adsorption with a good accuracy (Fig. 3) [12].

In situ measurements and the analysis of the magnetoconductance (MC) and the Hall resistance (HR) of 20-BL Bi(111) films at the variation of a magnetic field directed perpendicularly to the film surface allowed us to obtain numerical characteristics of the charge carrier scattering processes in the surface states: the mobilities, relaxation times, and concentration of electrons and holes in the surface states, which reflect the charge redistribution between them and adatoms.

As the first approximation, the charge redistribution between Bi adatoms and Bi(111) surface states can be neglected. Therefore, a reduction of the conductance at the Bi adsorption (Fig. 3) is mainly resulted from a reduction of the charge carrier mobility. This conclusion is confirmed by experimental magnetic-field dependences of MC, $G(B) - G(0) = F(B)$, measured at various coverages $\delta\Theta$ of adsorbed Bi, the curvature of which decreases, as $\delta\Theta$ increases (Fig. 4, *a*). At the same time, the square-law functional dependence on B, which corresponds to the

conclusions of the classical magnetotransport theory for charge carriers of two types [34],

$$G_{\text{class}}(B) = G(0) \frac{1 + (1-c)^2 \dfrac{\mu_n^2 \mu_p^2}{(\mu_n^+ c\mu_p)^2} B^2}{1 + \mu_n \mu_p \dfrac{\mu_p + c\mu_n}{\mu_n + c\mu_p} B^2}, \qquad (3)$$

where μ_n and μ_p are the mobilities of electrons and holes, respectively, and $c = p/n$ is the ratio between their concentrations, p and n, survives.

The magnetic-field dependences of the specific HR (Fig. 4, *b*) were registered simultaneously with the MC ones (Fig. 4, *a*). At the same time, they were calculated by the formula

$$\rho_{\text{H}}(B) = (\pi/\ln 2)(U_{\text{H}}/I),$$

where U_{H} is the Hall voltage, and I the measured current. The classical theory of magnetotransport with carriers of two types describes the specific HR by the formula [34]

$$\rho_{\text{H}}(B) = -\frac{B}{|e|} \frac{n\mu_n^2 - p\mu_p^2 + (n-p)\mu_n^2\mu_p^2 B^2}{(n\mu_n + p\mu_p)^2 + (n-p)^2\mu_n^2\mu_p^2 B^2}. \qquad (4)$$

The approximation of experimental data obtained for the MC (Fig. 4, *a*) and the HR (Fig. 4, *b*) by the classical magnetotransport formulas (3) and (4) allowed us to numerically evaluate the mobilities of carriers in Bi(111) surface electronic states and their variations with a change of the coverage degree by adsorbed Bi (Fig. 4, *c*). In so doing, we assumed the surface concentrations of electrons, $n = 3 \times 10^{12}$ cm^{-2}, and holes, $p = 4 \times 10^{12}$ cm^{-2}, to be fixed.

A reduction of the charge carrier mobility at higher coverages $\delta\Theta$ was observed at the adsorption of all examined impurity atoms, which directly corresponds to the diminishing of the mean free path of carriers at their non-coherent scattering by adsorbed impurities. Using the numerical data for the mobility and the formula

$$G_{\text{surf}}(\delta\Theta) = (\pi/\ln 2)e(n\mu_n(\delta\Theta) + p\mu_p(\delta\Theta)),$$

the surface conductances of Bi(111) films at various coverages by adsorbed Bi atoms were calculated (Fig. 4, *c*). The agreement between the calculated ($\Delta G/G_0|_{0.04\text{ ML}} = 0.37$; Fig. 4, *c*) and measured ($\Delta G/G_0|_{0.04\text{ ML}} = 0.22$; Fig. 3, *b*) values confirms
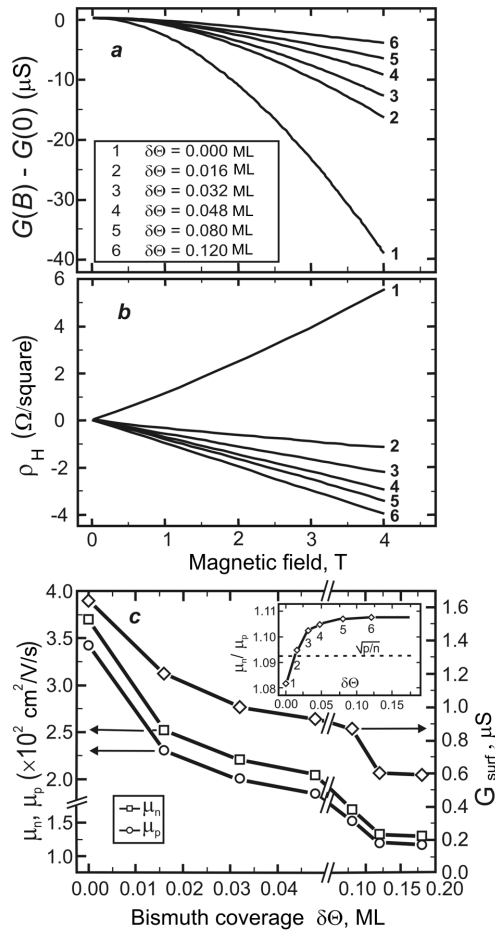
Fig. 5. Magnetic-field dependences of the magnetoconductance G (a) and the specific Hall resistance ρ_H (b) for various coverages $\delta\Theta$ of Fe adsorbed at $T = 10$ K on the 20-ML Bi(111) film surface [11]. Dashed curve shows the approximation of $G(B)$ by the square-law function (3). The approximation of $G(B)$ by a combination of formulas of the WL theory [36] and the classical magnetotransport theory [34] is shown in the inset

Fig. 4. Dependences of the magnetoconductance G (a) and the specific Hall resistance ρ_H (b) on the magnetic field for various coverages $\delta\Theta$ of Bi adsorbed at $T = 10$ K on the 20-ML Bi(111) film surface; (c) the mobilities of electrons (μ_n, squares) and holes (μ_p, circles) (the left ordinate axis) and the surface conductance $G = \sigma\pi/\ln 2$ (diamonds, the right ordinate axis) obtained from magnetotransport data (panels a and b). The dependence of μ_n/μ_p on $\delta\Theta$) illustrating the origin of different slopes in the ρ_H-curves is shown in the inset [11]

Fig. 6. (a) Mobilities of electrons (μ_n, squares) and holes (μ_p, circles) in the surface states of Bi(111) covered with Fe adatoms, (b) the corresponding concentrations of electrons (n, triangles) and holes (p, circles) obtained from the MC and HR data (Fig. 5) [11]

once more the conclusion about the dominant contribution of surface states to the electron transport in thin Bi(111) films. Note also that the inversion of the HR sign at the Bi adsorption is related only to a change of the ratio between the electron and hole mobilities at their constant concentrations (Fig. 4, b). In the approximation of low magnetic fields, the specific HR depends linearly on B (Eq. (4)), and the sign of ρ_H is positive, if $\mu_n/\mu_p < \sqrt{p/n} = 1.09$ or negative otherwise (Fig. 5, c).
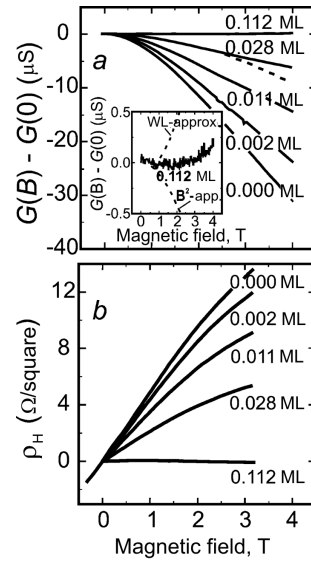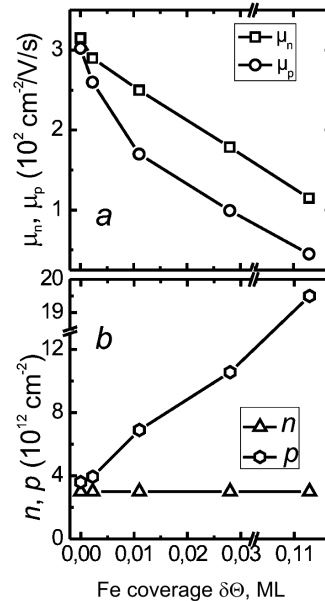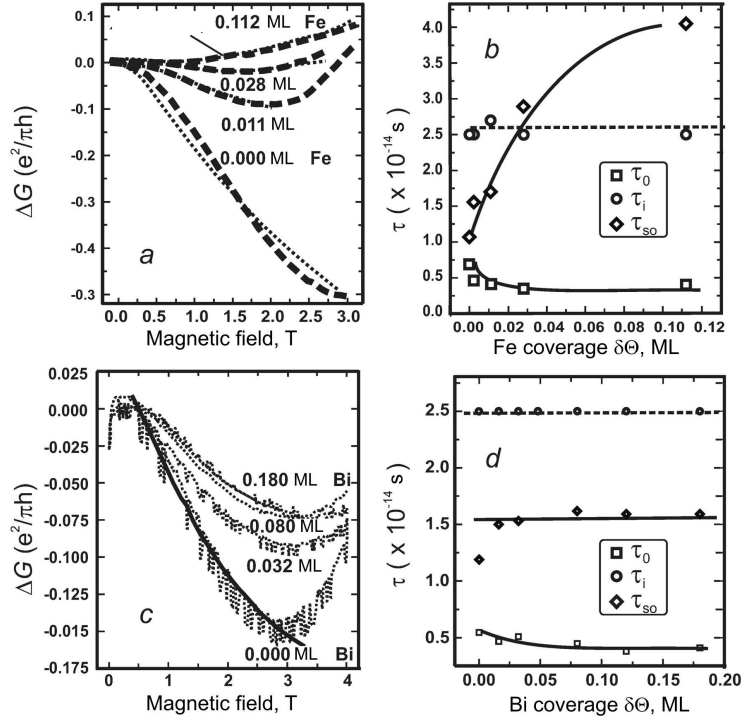
Fig. 7. "Quantum component" of the magnetoconductance ($\Delta G = G - G_{\text{class}}$) in 20-ML Bi(111) films with various coverages of adsorbed Fe (a) and Bi (c); examples of approximations in the framework of the Hikami theory [36] are shown. (b) and (d) give the dependences of the elastic (τ_0), inelastic (τ_i), and spin-orbit (τ_{so}) scattering times on the corresponding adsorbed atom coverage calculated from the relevant approximations [11]

A comparison of the magnetotransport measurement results for Bi(111) films covered with Bi (Fig. 4) and Fe (Fig. 5) adatoms in the same interval of coverages by adsorbates shows that the MC diminishes more rapidly in the case of magnetic Fe adsorption. Moreover, in the latter case, deviations from the square-law dependence of MC and even its enhancement are observed (Fig. 5), which testifies to the suppression of the weak antilocalization (WAL) effect and the strengthening of the weak localization (WL) one [35], which are discussed below. The self-consistent approximation of the MC and HR dependences (Fig. 5) by formulas (3) and (4) made it possible to find the dependences of the charge carrier mobilities and the concentrations in surface states on the coverage degree with Fe adatoms (Fig. 6). It is evident that a reduction in the mobility owing to the Fe adsorption is approximately twice as large as that caused by Bi adatoms. Moreover, Fe adatoms are acceptors, and each of them takes away a charge approximately equal to $0.5e^-$ from Bi(111) surface states.

Conclusions about the efficiency of the charge carrier scattering were drawn according to the analysis of the "quantum correction" to MC. This correction characterizes the WL effect, which consists in the localization of charge carriers owing to the constructive interference of electron waves at the multiple processes of elastic scattering along a closed trajectory, and the WAL effect, which consists in the suppression of the WL effect as a result of the destructive interference of electron waves in systems with strong spin-orbit coupling. The correction to the conductance was obtained by subtracting the "classical" MC component G_{class} (Eq. (3)) from experimental data.

The dependences $\Delta G = G - G_{\text{class}} = F(B)$ for Bi(111) films covered with Fe and Bi adatoms to various coverages are shown in Figs. 7, a and c, respectively. It is evident that the WAL effect dominates un the case of the film with the atomically clean surface (a reduction of the difference $G - G_{\text{class}}$, as the magnetic field increases, testifies to the suppression of this effect). The adsorption of Bi atoms (at least

to the coverage $\delta\Theta \approx 0.18$ ML) does not qualitatively change the behavior of $G - G_{\text{class}}$ (Fig. 7, c), whereas the Fe coverages with $\delta\Theta > 0.3$ ML change the sign of this quantity, which evidences the predominance of the WL effect suppressed by the magnetic field (Fig. 7, a). Taking into account that both Bi and Fe atoms are responsible for a reduction of the mean free path of charge carriers in the surface states, we may draw conclusion that the transition between the WAL and WL regimes, which is observed at the Fe adsorption, is unambiguously associated with a considerable magnetic moment of adatoms.

The approximation of the dependences $G - G_{\text{class}} = F(B)$ using the formulas of the Hikami theory [36], which describes the behavior of MC in 2D systems, for which the WL and WAL processes are essential (Figs. 7, a and c), allowed us to determine the relaxation times that characterize the various mechanisms of charge carrier scattering in the Bi(111) surface states – elastic τ_0, inelastic τ_i, and spin-orbit τ_{so} ones – for various coverages by adsorbed atoms (see details in work [10]). Those results (Figs. 7, b and d) demonstrate a gradual reduction of the elastic scattering time τ_0 when the coverages of both adsorbates increase (this is expected in view of the data presented in Fig. 4). However, the most remarkable effect is the fourfold increase of the spin-orbit scattering time τ_{so} caused by the Fe adsorption, whereas it remains almost invariable at the Bi adsorption. Hence, the WAL effect survives at all concentrations of adsorbed Bi atoms used in the experiment, and the parameters of the strong spin-orbit coupling in surface electronic states, which are split owing to the Rashba

Relative cross-sections of charge carrier scattering in Bi(111) surface states by various adatoms ($\sigma_{\text{adatom}}/\sigma_{\text{Bi}}$), the ratio $\tau_{\text{so}}(0.1\ \text{ML})/\tau_{\text{so}}(0\ \text{ML})$ between the times of the spin-orbit scattering (for Cr, $\tau_{\text{so}}(0.035\ \text{ML})/\tau_{\text{so}}(0\ \text{ML})$), and the average charge change of adatoms at the adsorption (Δq)

Adatom	$\dfrac{\sigma_{\text{adatom}}}{\sigma_{\text{Bi}}}$	$\dfrac{\tau_{\text{so}}(0.1\ \text{ML})}{\tau_{\text{so}}(0\ \text{ML})}$	$\Delta q(\text{e}^-/\text{atom})$	Source
Bi	~1	~1	~0	[11]
Co	~2	~4	−0.6	[11]
Fe	~2	~4	−0.5	[11]
Tb	~2.7	~3	0.05	[13]
Cr	~6	~4	0.03	[14]
Sb	~1	–	<0	[–]

effect, remain constant. For comparison, Table contains the parameters for the charge carrier scattering in Bi(111) surface states by various adatoms and for the charge redistribution between those adatoms and Bi(111) surface states (the treatment of experimental data for adsorbed Sb has not been finished yet).

4. Conclusions

In this review, we summarized the results of two experimental series, in which the physical effects related to the surface scattering of charge carriers and the properties of surface electronic states in metals were studied with the help of methods based on magnetotransport measurements. The main result obtained in the first experimental series is the increase of the specularity degree for the scattering of charge carriers at the W(110) and Mo(110) surfaces, when the transitions between the bulk and surface electronic states stimulated by the surface scattering are forbidden. This occurs owing to an adsorption-induced modification of the surface electronic structure. Those experiments made it possible to evaluate the contribution of surface-state charge carriers (about 5%) to the macroscopic magnetoconductance of metal plates, which are under the conditions of the static skin effect. A promising continuation of the researches can be similar experiments on epitaxial nanofilms of refractory metals, which are real candidates to be used in electronics [37].

In the second experimental series, the mechanisms of charge carrier scattering in spin-split surface electronic states of Bi(111) epitaxial nanofilms ($d \approx 8$ nm), in which the surface conductance dominates at low temperatures owing to the "semimetal-semiconductor" transition in the bulk, were studied. Our experiments confirmed that the charge carriers in those surface states are protected from the backward scattering (as it follows from the time-inversion symmetry), and the adsorption to low (<0.1 ML) concentrations of nonmagnetic (Bi, Sb) atoms leads only to the non-coherent carrier scattering. On the other hand, the adsorbed magnetic atoms (Co, Fe, Cr, Tb) locally break the time-inversion symmetry and provoke the coherent backward scattering of charge carriers (although this scattering channel does not dominate). The fact that a critical concentration of magnetic adsorbate is required to obtain the weak localization effect for charge carriers tes-

tifies to a simplified character of the spin-flip scattering model in systems with strong spin-orbit coupling. The problem concerning the lower scattering ability of $4f$-adatoms (Tb), which possess a higher magnetic moment, in comparison with $3d$-adatoms (Co, Fe, and Cr) remains unresolved. In those experiments, it was also found that the charge redistribution between surface states and adatoms (see Table) is an extremely important effect, which not only affects the surface conductance, but also can change the magnetic moment of adatoms and the surface electronic structure. In this sense, the independent measurements of concentration variations for the charge carriers in surface electronic states at the adsorption, e.g., by registering the variation of surface potential, would be undoubtedly useful. In addition, in order to clarify the microscopic mechanism of scattering of Bi surface states, the further researches concerning the registration and the analysis of the symmetry of interference patterns obtained at the scattering of Bi surface states by adsorbed magnetic and nonmagnetic atoms and molecules, are required. Some of them were started in the last years [38–40].

1. A. Fert, Rev. Mod. Phys. **80**, 1517 (2008); P.A. Grünberg, Rev. Mod. Phys. **80**, 1531 (2008).

2. J.E. Moore, Nature **464**, 194 (2010).

3. P. Roushan, J. Seo, C.V. Parker, Y.S. Hor, D. Hsieh, D. Qian, A. Richardella, M.Z. Hasan, R.J. Cava, and A. Yazdani, Nature **460**, 1106 (2009).

4. S. Xiao, D. Wei, and X. Jin, Phys. Rev. Lett. **109**, 166805 (2012).

5. O.A. Panchenko, P.P. Lutsishin, and S.V. Sologub, Progr. Surf. Sci. **69**, 193 (2002).

6. Ph. Hofmann, and J.W. Wells, J. Phys.: Condens. Matter **21**, 013003 (2009).

7. O.A. Panchenko and S.V. Sologub, Phys. Rev. B **71**, 193401 (2005).

8. O.A. Panchenko, S.V. Sologub, and I.V. Bordenjuk, Funct. Mater. **12**, 742 (2005).

9. O.A. Panchenko, S.V. Sologub, and I.V. Bordenjuk, Surf. Sci. **605**, 1287 (2011).

10. D. Lükermann, S. Sologub, H. Pfnür, and C. Tegenkamp, Phys. Rev. B **83**, 245425 (2011).

11. D. Lükermann, S. Sologub, H. Pfnür, C. Klein, M. Horn-von-Hoegen, and C. Tegenkamp, Phys. Rev. B **86**, 195432 (2012).

12. S. Sologub, D. Lükermann, H. Pfnür, and C. Tegenkamp, Phys. Rev. B **88**, 115412 (2013).

13. P. Kröger, S. Sologub, C. Tegenkamp, and H. Pfnür, J. Phys.: Condens. Matter **26**, 22502 (2014).

14. A.F. Andreev, Usp. Fiz. Nauk **105**, 113 (1971).

15. P.P. Lutsishin, T.N. Nakhodkin, O.A. Panchenko, and Yu.G. Ptushinskii, Zh. Eksp. Teor. Fiz. **82**, 1306 (1982).

16. M.Ya. Azbel and V.G. Peschanskii, Zh. Eksp. Teor. Fiz. **49**, 572 (1965).

17. A.G. Kundzich, P.P. Lutsishin, O.A. Panchenko, S.V. Sologub, and V.F. Shpagin, Surf. Sci. **248**, 207 (1991).

18. M. Arnold, S. Sologub, G. Hupfauer, P. Bayer, W. Frie, L. Hammer, and K. Heinz, Surf. Rev. Lett. **4**, 1291 (1997).

19. K. Jeong, R.H. Gaylord, and S.D. Kevan, Phys. Rev. B **39**, 2973 (1989).

20. E. Rotenberg and S.D. Kevan, Phys. Rev. Lett. **80**, 2905 (1998).

21. Yu.F. Ogrin, V.N. Lutskii, and M.I. Elinson, Pis'ma Zh. Eksp. Teor. Fiz. **3**, 114, 1996.

22. V.B. Sandomirskii, Zh. Eksp. Teor. Fiz. **52**, 158 (1967).

23. C.A. Hoffman, J.R. Meyer, F.J. Bartoli, A. Di Venere, X.J. Yi, C.L. Hou, H.C. Wang, J.B. Ketterson, and G.K. Wong, Phys. Rev. B **51**, 5535 (1995).

24. C.A. Hoffman, J.R. Meyer, F.J. Bartoli, A. Di Venere, X.J. Yi, C.L. Hou, H.C. Wang, J.B. Ketterson, and G.K. Wong, Phys. Rev. B **48**, 11431 (1993).

25. T. Hirahara, I. Matsuda, S. Yamazaki, N. Miyata, S. Hasegawa, and T. Nagao, Appl. Phys. Lett. **91**, 202106 (2007).

26. G. Jnawali, Th. Wagner, H. Hattab, R. Möller, A. Lorke, and M. Horn-von Hoegen, e-J. Surf. Sci. Nanotechnol. **8**, 27 (2010).

27. E.I. Rashba, Fiz. Tverd. Tela **2**, 1224 (1960); A.Yu. Bychkov and E.I. Rashba, Pis'ma Zh. Eksp. Teor. Fiz. **39**, 66 (1984).

28. Y.M. Koroteev, G. Bihlmayer, J.E. Gayone, E.V. Chulkov, S. Blügel, P.M. Echenique, and Ph. Hofmann, Phys. Rev. Lett. **93**, 046403 (2004).

29. J. Henk, M. Hoesch, J. Osterwalder, A. Ernst, and P. Bruno, J. Phys.: Cond. Mat. **16**, 7581 (2004).

30. Ph. Hofmann, J.E. Gayone, G. Bihlmayer, Yu.M. Koroteev, and E.V. Chulkov, Phys. Rev. B **71**, 195413 (2005).

31. H. Dil, J. Phys.: Cond. Mat. **21**, 403001 (2009).

32. M. Horn-von Hoegen, Z. Kristallogr. **214**, 591 (1999).

33. J.A. Venables, G.D.T. Spiller, and M. Hanbücken, Rep. Prog. Phys. **47**, 399 (1984); H. Brune, Surf. Sci. Rep. **31**, 125 (1998).

34. A.B. Pippard, *Magnetoresistance in Metals* (Cambridge Univ. Press, Cambridge, 1989).

35. G. Bergmann, Phys. Rep. **107**, 1 (1984).

36. S. Hikami, A.I. Larkin, and Y. Nagaoka, Prog. Theor. Phys. **63**, 707 (1980).

37. D. Choi, C.S. Kim, D. Naveh, S. Chung, A.P. Warren, N.T. Nuhfer, M.F. Toney, K.R. Coffey, and K. Barmak, Phys. Rev. B **86**, 045432 (2012).

38. M.C. Cottin, C.A. Bobisch, J. Schaffert, G. Jnawali, A. Sonntag, G. Bihlmayer, and R. Möller, Appl. Phys. Lett. **98**, 022108 (2011).

39. A. Stróżecka, A. Eiguren, and J.I. Pascual, Phys. Rev. Lett. **107**, 186805 (2011).

40. M.C. Cottin, C.A. Bobisch, J. Schaffert, G. Jnawali, G. Bihlmayer, and R. Möller, Nano Lett. **13**, 2717 (2013).

С.В. Сологуб, І.В. Борденюк, К. Тегенкамп, Х. Пфнюр

ПОВЕРХНЕВЕ РОЗСІЮВАННЯ НОСІЇВ
СТРУМУ І ПОВЕРХНЕВІ ЕЛЕКТРОННІ СТАНИ

Р е з ю м е

Наведений огляд експериментальних досліджень розсіювання носіїв струму на атомночистих і вкритих моношарами водню (дейтерію) поверхнях Mo(110) і W(110), яке відбувається за участю поверхневих електронних станів, а також механізмів розсіювання носіїв струму спін-поляризованих поверхневих електронних станів епітаксійних наноплівок Bi(111) з атомночистою і вкритою надмалими покриттями магнітних і немагнітних адатомів поверхнею.